Absolute Rate Constant and Product Branching Fractions for the Reaction between F and C_2H_4 at $T = 202-298$ K

Fred L. Nesbitt[†]
Department of Natural Sciences, Coppin State College, Baltimore, Maryland 21216

R. Peyton Thorn, Jr.*[,‡] **and Walter A. Payne, Jr.**[§]
Laboratory for Extraterrestrial Physics, NASA/Goddard Space Flight Center, Greenbelt, Maryland 20771

D. C. Tardy*[,||]
Department of Chemistry, University of Iowa, Iowa City, Iowa 52242

Received: January 12, 1999; In Final Form: April 15, 1999

The discharge-flow kinetic technique coupled to mass-spectrometric detection has been used to determine the variable-temperature dependence of the rate constant and product branching fractions for the reaction between F(^{2}P) and C_2H_4 at $P = 1$ Torr nominal pressure (He). The reaction was studied at $T = 202$ and 236 K by monitoring the decay of C_2H_4 in the presence of a large excess of F(^{2}P). The overall rate coefficients were determined to be $k_1(202\ \text{K}) = (1.7 \pm 0.4) \times 10^{-10}$ cm^3 molecule^{-1} s^{-1} and $k_1(236\ \text{K}) = (2.1 \pm 0.5) \times 10^{-10}$ cm^3 molecule^{-1} s^{-1} with the quoted uncertainty representing total errors. Further, the branching fractions for the two observed reaction channels F + $C_2H_4 \rightarrow C_2H_3$ + HF (1a) and F + $C_2H_4 \rightarrow C_2H_3F$ + H (1b) were determined by quantitatively measuring the yield of C_2H_3F under conditions of excess C_2H_4. The stabilized adduct, C_2H_4F, was not detected at $T = 202$ K. The derived branching fractions were $\Gamma_{1a}(202\ \text{K}) = 0.25 \pm 0.09$, $\Gamma_{1b}(202\ \text{K}) = 0.75 \pm 0.16$, and $\Gamma_{1a}(236\ \text{K}) = 0.27 \pm 0.13$, and $\Gamma_{1b}(236\ \text{K}) = 0.73 \pm 0.20$, where the quoted uncertainty represents total errors. By inclusion of $k_1(298\ \text{K}) = (3.0 \pm 0.8) \times 10^{-10}$ cm^3 molecule^{-1} s^{-1}, a revised value that used data from our previous study and $\Gamma_{1a}(298\ \text{K}) = 0.35 \pm 0.04$ and $\Gamma_{1b}(298\ \text{K}) = 0.65 \pm 0.04$ from a laser photolysis/photoionization mass spectrometry study, we obtain the Arrhenius expressions $k_{1a}(T) = (7.5 \pm 4.0) \times 10^{-10} \exp[(-1.2 \pm 0.3)/(RT)]$ and $k_{1b}(T) = (5.2 \pm 1.0) \times 10^{-10} \exp[(-0.6 \pm 0.1)/(RT)]$ in units of cm^3 molecule^{-1} s^{-1} for k and in units of kcal mol^{-1} for activation energy. The quoted uncertainty represents total errors at 1σ precision errors plus 15% systematic errors. RRKM calculations have shown that the critical energy for H addition to C_2H_3F is less than 6 kcal mol^{-1} larger than that for the addition of F to C_2H_4 and that the competitive decomposition of chemically activated C_2H_4F radicals favor C−H bond rupture by a factor greater than 1000 over that for C−F bond rupture.

Introduction

The kinetics of small C_2 radicals such as vinyl (C_2H_3) have implicit importance in the atmospheric chemistry of the outer planets,[1] in high-temperature chemistry of combustion processes,[2] and in ultralow-temperature chemistry of dense interstellar clouds.[3] These C_2 radical species are generated either by thermal or vacuum ultraviolet dissociation from a stable precursor molecule or by chemical reaction. For example, in Titan's atmosphere, C_2H_3 is produced by the termolecular association reaction of H with C_2H_2.[1,4] Once produced in such systems, these radicals serve to interconvert hydrocarbon species.[1]

The reaction of fluorine atoms with hydrocarbons is an important laboratory source of hydrocarbon radicals. For the reaction of fluorine atoms with alkanes only one pathway is available: a H atom abstraction with the production of HF and an alkyl radical.[5] The high reactivity of F atoms leads to rate coefficients that typically are at the collision rate,[6] e.g., for the F + C_2H_6 reaction, $k(298\ \text{K}) = 2.2 \times 10^{-10}$ cm^3 molecule^{-1} s^{-1}.[7] Although the prompt radical generation is very desirable to consume the initial F present and thus prevent secondary chemistry, the high reactivity of F also leads to a low selectivity, i.e., multiple pathways. In contrast to the alkanes, the reaction of fluorine atoms with the an alkene, e.g., C_2H_4, can occur by two processes: (1) direct H atom abstraction to form HF and the corresponding free radical, (2) addition of fluorine atoms to the double bond to yield an energetic adduct, C_2H_4F*.[8] The C_2H_4F* adduct can then decompose through the loss of a H atom to form vinyl fluoride, C_2H_3F, or it can be collisionally stabilized to form an adduct-like product C_2H_4F.[9,10] This mechanism results in three possible exothermic product pathways:

$$F(^2P) + C_2H_4 \rightarrow C_2H_3 + HF \quad (1a)$$

$$\rightarrow [C_2H_4{-}F]^* \rightarrow C_2H_3F + H \quad (1b)$$

$$\rightarrow [C_2H_4{-}F]^* + M \rightarrow C_2H_4F + M^* \quad (1c)$$

Thus, the F + C_2H_4 reaction system illustrates the three categories of a bimolecular reaction: a metathesis (abstraction),

* To whom correspondence should be sent.
[†] Email: fnesb29280@aol.com.
[‡] Email: ysrpt@lepvax.gsfc.nasa.gov.
[§] Email: u1wap@lepvax.gsfc.nasa.gov.
[||] Email: dwight-tardy@uiowa.edu.

10.1021/jp9901747 CCC: $18.00
Published on Web 05/22/1999

a displacement (addition followed by decomposition), and an association (addition followed by stabilization) reaction.[11]

Previous reaction dynamic studies have shown that the F + C_2H_4 reaction proceeds by parallel abstraction and addition mechanisms.[8] Specifically, a crossed molecular beam study of F atoms with C_2H_4 and C_2D_4 by Parson and Lee[8] determined that the addition adduct was a long-lived complex, which after several rotational periods eventually released a H atom and vinyl fluoride. This study also determined that the abstraction channel produced a highly vibrationally excited DF (populating $v' = 2$, the highest thermochemically accessible level) and a vinyl radical with very little internal energy. The reaction of F atoms with C_2H_4 has also been extensively studied by infrared chemiluminescence techniques.[12−15] A chemiluminescence study[12] and a high collision energy (2.3−12.1 kcal mol^{-1}) crossed molecular beam study[16] have shown that the energy in the vinyl fluoride product from reaction 1b was not completely randomized because of the exit channel barrier of 5−6 kcal mol^{-1}. A more recent, lower collision energy (0.8−2.5 kcal mol^{-1}) crossed molecular beam study[17] has established an upper limit of 0.8 kcal mol^{-1} as the potential energy barrier to F atom addition to C_2H_4.

Despite the intense interest from the reaction dynamics viewpoint in the F + C_2H_4 reaction system, there have been few bulk gas-phase kinetic and product branching fraction measurements. To date, there are two relative rate measurements[18,19] and only one absolute rate measurement[20] at $T = 298$ K for reaction 1 reported in the literature. Milstein et al.[18] reported a relative rate of 0.82 ± 0.02 in 4000 Torr of SF_6 for addition reaction via reaction 1c relative to

$$F(^2P) + C_2H_2 \rightarrow C_2H_2F \qquad (2)$$

and Smith et al.[19] reported a relative rate of 0.52 ± 0.08 for only the abstraction reaction 1a, k_{1a}, relative to

$$F(^2P) + CH_4 \rightarrow HF + CH_3 \qquad (3)$$

in ∼1 Torr Ar carrier gas. The previous absolute rate coefficient measurement,[20] performed in this laboratory, yielded the result $k_1(\text{total}) = (2.7 \pm 0.5) \times 10^{-10}$ cm^3 molecule^{-1} s^{-1} using the same technique and similar conditions described below. The relative rate measurement of Milstein et al.[18] is consistent with our previous k_1(total) value when combined with a value of $\Gamma_{1c} = k_{1c}/k_1(\text{total}) \cong \Gamma_{1b} = k_{1b}/k_1(\text{total}) = 0.65$ from ref 21 and a recent measurement of k_2.[20] As discussed later, the total addition channel rate coefficient, $k_{add} = k_{1b} + k_{1c}$, is believed to be pressure-independent, and therefore, the only effect of pressure is the partitioning between the stabilization and decomposition pathways of the adduct. Thus, the relative measurement of k_{1c} by Milstein et al.[18] at high pressure can approximate a measurement of k_{1b} at low pressure. The other relative rate measurement by Smith et al.[19] yielded only fair agreement with our previous k_{1a} value, which was calculated from a value of $\Gamma_{1a} = k_{1a}/k_1(\text{total}) = 0.35$ from ref 21 and our previous k_1(total) value.[20]

There have been three previous product branching studies carried out at $T = 295-298$ K over a wide range of pressures and carrier gases: in 100−4000 Torr of SF_6 and 240−1580 Torr of CF_4,[9] in 0.7 Torr of He,[21] and in 2×10^{-4} Torr of C_2H_4.[13] These three studies are in good agreement with one another and have shown that the addition processes in this reaction, channels 1b and 1c, occur about twice as frequently as does abstraction. The most recent and accurate measurement of $\Gamma_{1b} = 0.65$ (±0.06) was obtained by Slagle and Gutman[21] using a pulsed IR laser photolysis−photoionization mass spectrometry technique. In this study, the F atoms were generated by IR multiple photon decomposition of C_6F_5Cl, and the absolute branching fraction was determined from measurements of both the C_2H_4 depletion and the C_2H_3F product formation. In an earlier study, Moehlmann and McDonald[13] measured the integrated HF infrared chemiluminescence and after deconvolution of the data determined an addition−decomposition/abstraction cross-section ratio of 3, i.e., $\Gamma_{1b} = 0.75$. The accuracy of this value is not known because of a need to assume populations of the $v = 0$ state of HF and the difficulty in determining absolute Einstein coefficients for C_2H_3F. In the first product branching study, which measured the yields of the ^{18}F-containing product compounds by radio gas chromatography, Williams and Rowland[9] reported a total addition channel branching fraction, $\Gamma_{add} = \Gamma_{1b} + \Gamma_{1c}$, of 0.65.

However, there has not been any kinetic or product branching fraction studies at low temperatures. The objective of this study is to make direct measurements of the absolute rate constant and product branching fractions of reaction 1 as a function of temperature. Measurements were made using the discharge flow mass spectrometric technique at 1 Torr total pressure. These studies confirm that reaction 1 is a convenient and quantitative laboratory source of the C_2H_3 radical over the temperature range $T = 202-298$ K.

Experimental Section

Discharge Flow Reactor. All experiments were performed in a Pyrex flow tube 60 cm long and 2.8 cm in diameter, the inner surface of the flow tube being lined with Teflon FEP. The flow tube was coupled via a two-stage stainless steel collision-free sampling system to a recently installed computer-controlled quadrupole mass spectrometer (Merlin mass spectrometer, ABB Extrel Corp.) that was operated at low electron energies (typically less than 20 eV). Ions were detected by an off-axis conversion dynode/channeltron multiplier (Detector Technology Corp.). The flow tube has a Pyrex movable injector for the introduction of the C_2H_4 reactant, which could be changed from a distance between 2 and 40 cm from the sampling pinhole. Helium carrier gas was flowed at 945 sccm into the reaction flow tube through ports at the rear of the flow tube. All gas flows were measured and controlled by mass flow controllers (MKS Instruments). At a typical total pressure of 1 Torr the linear flow velocity was between 2360 and 3000 cm s^{-1}. This system has been described in detail previously.[22]

Atomic F Production and Titration. Fluorine atoms were generated by passing molecular fluorine (ca. 5% diluted in helium) or CF_4 (ca. 10% diluted in helium) through a sidearm at the upstream end of the flow tube that contained a microwave discharge (∼50 W, 2450 MHz, Opthos Instruments). The discharge region consisted of a $^3/_8$ in. ceramic tube coupled to a glass discharge arm. When CF_4 was used, a recombination volume was placed downstream from the microwave discharge to allow CF_x to recombine. The volume was 10 cm in length, 7 cm in diameter Pyrex glass, giving a residence time of ca. 60 ms.

The concentration of fluorine atoms in the kinetic studies was determined by measuring the Cl_2 consumption in the fast titration reaction

$$F + Cl_2 \rightarrow FCl + Cl \qquad (4)$$

$$k_4(298\text{ K}) = 1.6 \times 10^{-10}\text{ cm}^3\text{ molecule}^{-1}\text{ s}^{-1}\text{ (ref 23)}$$

With Cl_2 in excess, the F atom concentration was determined

by measuring the decrease in the Cl_2^+ signal ($m/z = 70$) at an electron energy of ~14 eV when the discharge was initiated. The dilute Cl_2/He mixture was admitted via the movable injector. The position of the injector was chosen to ensure that reaction 4 went to completion and that the position was close to the middle of the decay range for C_2H_4 under reaction conditions. The absolute F concentration is given by $[F] = [Cl_2]_{Disc.Off} - [Cl_2]_{Disc.On} \equiv (\Delta Cl_2 \text{ signal})[Cl_2]_{Disc.Off}$. As discussed previously for N atom studies,[24] a number of precautions were taken in order to avoid systematic errors in this type of measurement. Typically, 80−96% of the F_2 was dissociated and initial F atom concentrations were $(1.0-5.0) \times 10^{12}$ molecule cm^{-3} for the kinetic studies. All F atom titrations for the kinetic studies were conducted in the presence of the same oxygen concentration as used in the decay experiments as discussed below.

For the product branching studies, the concentration of fluorine atoms was determined by measuring the decrease in the F_2^+ signal ($m/z = 38$) at an electron energy of ~20 eV when the discharge was initiated. This method was preferred because the product yield measurements were performed with the injector position between $d = 3$ and 5 cm from the sampling pinhole as discussed later in Results. If Cl_2 had been used as a titrant at this injector position, there would not be sufficient time for reaction 4 to go to completion. Separate experiments with the injector at 30 cm showed good agreement between the ΔCl_2 and the ΔF_2 methods. The absolute F concentration is given by $[F] = 2([F_2]_{Disc.Off} - [F_2]_{Disc.On}) \equiv 2(\Delta F_2 \text{ signal})[F_2]_{Disc.Off}$. Typically, 80−96% of the F_2 was dissociated and initial F radical concentrations were $(1.6-2.6) \times 10^{12}$ molecule cm^{-3} for the product branching studies.

In a few kinetic decay and product branching experiments at $T = 202$ K, CF_4 was used as the F atom precursor. Typically, 20−30% of the CF_4 was dissociated and the initial F atom concentrations were 1.8×10^{12} and 2.7×10^{12} molecule cm^{-3} for the kinetic studies and 4.25×10^{12} molecule cm^{-3} for the two product branching measurements. For the kinetic studies, the initial F concentration was determined by Cl_2 consumption as described above. However, for the product branching studies a ΔCF_4^+ signal decrease method (analogous to the ΔF_2^+ signal decrease method described above) could not be used, since there is not a CF_4^+ parent ion.[25] Instead, initial concentrations of F atoms were determined by measurements of the ClF ($m/z = 54$) generated in rapid reaction 4.[23] As in the Cl_2 consumption method, a dilute Cl_2/He mixture was admitted via the movable injector that was positioned to ensure that reaction 4 went to completion, typically at $d = 30$ cm. Although this injector position is 25 cm further upstream from where the product yield measurements were performed, previous experiments have shown that the F atom concentration profile in the flow tube is constant. This technique for measuring [F] by ClF formation, which avoids calibration with an external ClF reagent, has been thoroughly discussed by Appelman and Clyne.[23] This technique consists of two sequential measurements of the ClF signal. First, the Cl_2 reagent flow was set so that an excess of Cl_2 was present in the flow tube, $[Cl_2]_0/[F]_0 \geq 2$, therefore converting all F atoms to ClF. Then under the same mass spectrometer conditions and the same $[Cl_2]_0$, the $[F]_0$ was greatly increased, thereby consuming all the Cl_2 and the ClF signal measured. This second step determined the ClF signal calibration, since [ClF] product $= [Cl_2]_0$. Thus, the ClF signal from $F + Cl_2$ could be used to measure absolute F atom concentration in the $10^{11}-10^{13}$ molecule cm^{-3} range used in this product branching study.

Materials. Helium (99.9995%, Air Products) was drawn through a trap held at 77 K. F_2 (4.92% in helium, Air Products) and O_2 (99.999%, Scientific Gas Products, UHP) were used without further purification. Cl_2 (VLSI grade, Air Products), C_2H_4 (99%, Air Products), CF_4 (99.9%, Matheson), and C_2H_3F (98%, PCR Inc.) were degassed using repeated freeze−pump−thaw cycles at liquid nitrogen temperature.

Results

Kinetic Studies. The rate measurements were performed under pseudo-first-order conditions with $[F]_0 > [C_2H_4]_0$ and $[F]_0/[C_2H_4]_0$ values ranging from 8.4 to 13.6. The decay of C_2H_4 is given by the expression

$$\ln[C_2H_4]_t = -k_{obs}(d/v) + \ln[C_2H_4]_0 \quad (5)$$

where k_{obs} is the measured pseudo-first-order decay constant, d is the distance from the tip of the movable injector to the sampling pinhole, and v is the linear velocity. Linear least-squares analysis of plots of ln(C_2H_4 signal) at $m/z = 28$ vs contact time yielded the observed pseudo-first-order rate constant, $k_{obs.}$ Corrections (0.5−3%) were made to k_{obs} to account for axial diffusion to give k_{corr} according to the method of Lewis et al.[26] The diffusion coefficient for C_2H_4 in He was estimated to be $D = 288$ cm^2 s^{-1} and $D = 216$ cm^2 s^{-1} at $T = 236$ K and at $T = 202$ K, respectively. Corrections for radial diffusion were not necessary, since they were always smaller than axial diffusion.

As described previously,[20] nonlinearity in the C_2H_4 decay curves can be due to regeneration of ethylene via the rapid vinyl self-reaction

$$C_2H_3 + C_2H_3 \rightarrow C_2H_2 + C_2H_4 \quad (6)$$

$$k_6(298 \text{ K}) = 1.41 \times 10^{-10} \text{ cm}^3 \text{ molecule}^{-1} \text{ s}^{-1} \text{ (ref 27)}$$

Molecular oxygen, $[O_2]_0 = (3.6-3.9) \times 10^{14}$ molecule cm^{-3}, was added to scavenge C_2H_3.

$$C_2H_3 + O_2 \rightarrow HCO + H_2CO \quad (7)$$

$$k_7(298 \text{ K}) = 1.0 \times 10^{-11} \text{ cm}^3 \text{ molecule}^{-1} \text{ s}^{-1} \text{ (ref 28)}$$

In the presence of O_2 the observed first-order decays were strictly linear as required by eq 5 (see Figure 1). Possible contributions from the reaction

$$H + C_2H_4 + M \rightarrow C_2H_5 + M \quad (8)$$

$$k_8(1 \text{ Torr of He}) = 6.0 \times 10^{-14} \text{ cm}^3 \text{ molecule}^{-1} \text{ s}^{-1} \text{ (ref 29)}$$

to the depletion of C_2H_4 are negligible (<1%) under the conditions of the experiment.

To investigate the possibility of additional F atom loss processes, product observation experiments under the same pseudo-first-order conditions and at $T = 202$ and 236 K were performed by monitoring the fluoroethylene species C_2H_3F ($m/z = 46$), $C_2H_2F_2$ ($m/z = 64$), and C_2HF_3 ($m/z = 82$). The ionizer energy used was IE ≈ 14.0 eV, which is above the ionization energy of vinyl fluoride (IE = 10.36 eV), all three $C_2H_2F_2$ isomers, vinylidene fluoride (IE = 10.29 eV), (*Z*)-1,2-difluoroethylene (IE = 10.23 eV), (*E*)-1,2-difluoroethylene (IE = 10.21 eV), and trifluoroethylene (IE = 10.14 eV).[25] The results, shown in Figure 2, demonstrate that the consumption of C_2H_3F, which is the dominant product of reaction 1, occurs simultaneously and on approximately the same time scale as the C_2H_4

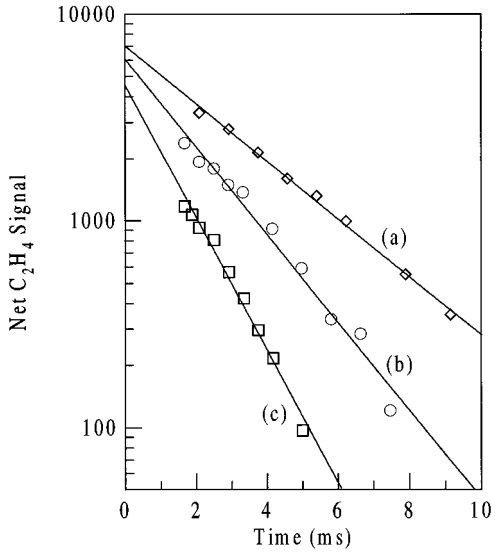

Figure 1. Plots of ln(C_2H_4 net signal) vs reaction time at $T = 202$ K and $P = 1$ Torr. Concentrations are in units of 10^{11} molecule cm^{-3}: $[F]_{mean}$ = (a) 19.6, (b) 26.8, (c) 45.4; $[C_2H_4]_0$ = (a) 1.56, (b) 2.44, (c) 4.91; $[O_2]_0$ = (a) 393, (b) 392, (c) 394. Solid lines are obtained from linear least-squares analyses and give the following pseudo-first-order C_2H_4 decay rates in units of s^{-1}: (a) 321, (b) 489, (c) 737. For clarity, traces a and c are shifted on the vertical axis; the actual net signal counts for trace a are twice that shown and for trace c are half that shown.

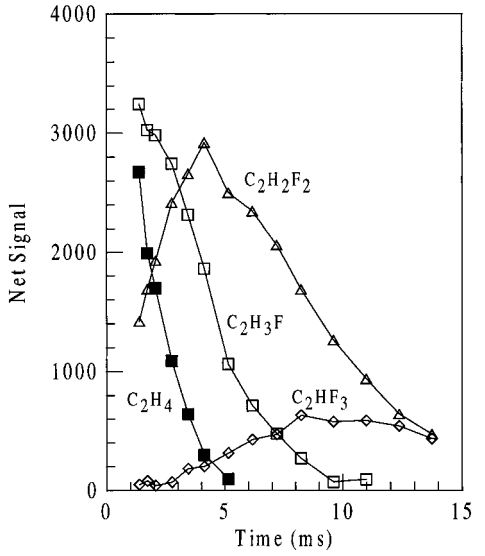

Figure 2. Plot of observed products at $T = 236$ K and $P = 1$ Torr with $[F]_0 > [C_2H_4]_0$. Concentrations are in units of molecule cm^{-3}: $[F]_0 = 3.45 \times 10^{12}$; $[C_2H_4]_0 = 3.40 \times 10^{11}$; $[O_2]_0 = 3.66 \times 10^{14}$.

decay. Furthermore, the increasing $C_2H_2F_2$ net signal correlates with the decreasing C_2H_3F net signal, implying that it is a major product of the F + C_2H_3F reaction at low pressures

$$F + C_2H_3F \rightarrow C_2H_2F_2 + H \quad (9a)$$

$$\rightarrow \text{other products} \quad (9b)$$

Although k_9 has not been measured here and has not been reported in the literature, its value should be between that of the Cl + C_2H_3F reaction in the high-pressure limit, 1.85×10^{-10} cm^3 molecule^{-1} s^{-1} at $T = 298$ K (ref 30), and that of reaction 1, $k_1(298\text{ K}) = 2.7 \times 10^{-10}$ cm^3 molecule^{-1} s^{-1}.[20] Similarly, the decay of the $C_2H_2F_2$ net signal correlates with the rise of the C_2HF_3 net signal, implying that it is a major product of the F + $C_2H_2F_2$ reaction

$$F + C_2H_2F_2 \rightarrow C_2HF_3 + H \quad (10a)$$

$$\rightarrow \text{other products} \quad (10b)$$

However, reaction 10 becomes significant only near the completion of reaction 1, and therefore, consumption of F by reaction 10 was neglected in determining $[F]_{mean}$.

To allow for the small depletion of F caused by reaction with C_2H_4 and with C_2H_3F as discussed above, measured concentrations of F were corrected according to

$$[F]_{mean} = [F]_0 - 0.5[C_2H_4]_0 - 0.5[C_2H_3F] \quad (11)$$

The value of $[C_2H_3F]$ resulting from reaction 1b can be approximated from the product branching fraction, Γ_{1b}, and the initial $[C_2H_4]_0$:

$$[C_2H_3F] = \Gamma_{1b}[C_2H_4]_0 \quad (12)$$

For the $T = 298$ K data, $\Gamma_{1b} = 0.65$ (ref 21) and thus

$$[F]_{mean} = [F]_0 - 0.825[C_2H_4]_0 \quad (13)$$

Since our results from the product branching studies showed that Γ_{1b} increased slightly with temperature, $[F]_{mean}$ values were slightly lower at $T = 202$ than at $T = 236$ and 298 K for the same $[C_2H_4]_0$ and $[F]_0$. The range for the correction was 6−13%.

This analysis to determine $[F]_{mean}$ via eqs 11 and 12 was applied to data from our previous study at $T = 298$ K.[20] The $[F]_{mean}$ values are lower than the initial $[F]_0$ by 16−31%. This is a larger correction than was used for the low-temperature data because lower $[F]_0/[C_2H_4]_0$ ratios were used in the previous study.

The bimolecular rate constant, k_1, is calculated from

$$k_{corr} = k_1[F]_{mean} + k_w \quad (14)$$

where k_w is a first-order rate constant that accounts for the loss of C_2H_4 on the walls of the flow tube or other sources. Table 1 summarizes the rate data and experimental condition for $T =$ 236 and 202 K. Figures 1 and 2 show typical first-order decays of C_2H_4 in excess [F]. Figure 3 shows the variation in the pseudo-first-order rate constant k_{corr} with $[F]_{mean}$ for reaction 1 at $T = 202-298$ K, respectively. A linear least-squares analysis of the data in Table 1 according to eq 14 gives a bimolecular rate constant of $k_1(236\text{ K}) = (2.1 \pm 0.5) \times 10^{-10}$ cm^3

TABLE 1: Summary of Rate Data for the F(^{2}P) + C_2H_4 Reaction at $T = 236$ K and $T = 202$ K[a]

temp K	atomic F precursor	$[F]_{mean}$ 10^{12} molecule cm^{-3}	$[C_2H_4]_0$ 10^{11} molecule cm^{-3}	k_{corr} s^{-1}
236	F_2	1.11	1.16	190
236	F_2	1.18	1.57	268
236	F_2	1.81	1.94	288
236	F_2	2.57	2.54	491
236	F_2	2.67	2.76	509
236	F_2	3.29	2.64	681
202	F_2	1.98	1.56	325
202	F_2	2.71	2.44	498
202	F_2	3.58	2.96	642
202	F_2	4.60	4.91	757
202	CF_4	1.61	2.80	299
202	CF_4	2.44	3.00	363

[a] Excess O_2 added to scavenge C_2H_3 radical and prevent regeneration of C_2H_4; see text.

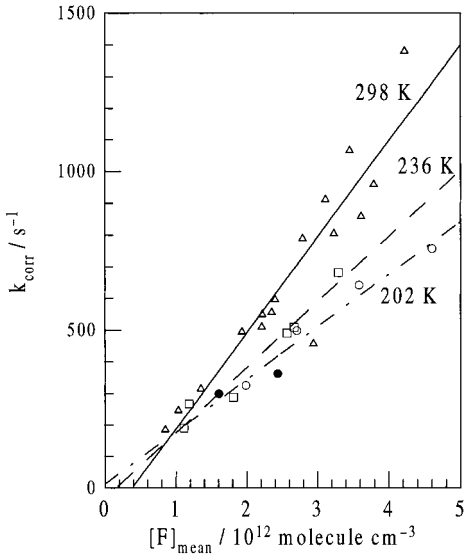

Figure 3. Summary plot of the corrected pseudo-first-order rate constant k_{corr} vs $[F]_{mean}$ at $P = 1$ Torr. The data points at $T = 202$, 236, and 298 K are indicated by circles, open squares, and open triangles, respectively. Open circle data points used F_2 as atomic F precursor. Solid circle data points used CF_4 as atomic F precursor. The lines are obtained from a linear least-squares analysis. At $T = 202$ K the slope of the dotted dashed line yields $k_1 = (1.66 \pm 0.41) \times 10^{-10}$ cm^3 molecule^{-1} s^{-1} and the intercept yields $k_w = +13 \pm 51$ s^{-1}. At $T =$ 236 K the slope yields $k_1 = (2.07 \pm 0.53) \times 10^{-10}$ cm^3 molecule^{-1} s^{-1} and the intercept yields $k_w = -32 \pm 54$ s^{-1}. At $T = 298$ K the slope yields $k_1 = (3.03 \pm 0.78) \times 10^{-10}$ cm^3 molecule^{-1} s^{-1} and the intercept yields $k_w = -114 \pm 106$ s^{-1}. Quoted uncertainties are 1σ plus 15%.

TABLE 2: Summary of Revised Rate Data for the F(^{2}P) + C_2H_4 Reaction at $T = 298$ K[a]

atomic F precursor	$[F]_{mean}$[b] 10^{12} molecule cm^{-3}	$[C_2H_4]_0$ 10^{11} molecule cm^{-3}	k_{corr} s^{-1}
F_2	2.35	9.31	559
F_2	0.84	4.33	188
F_2	1.93	7.23	498
F_2	2.94	9.20	461
F_2	3.79	14.3	963
F_2	3.61	12.9	862
F_2	4.22	17.8	1384
F_2	2.22	5.79	552
F_2	3.11	16.9	915
F_2	3.23	12.5	808
F_2	3.45	18.1	1068
F_2	2.79	10.6	794
F_2	2.21	6.55	513
F_2	1.03	3.60	250
F_2	1.35	4.38	318
F_2	2.40	5.72	599

[a] Original data from ref 20. Only $[F]_{mean}$ values have been revised. [b] Previous $[F]_{mean} = [F]_0 - 0.5[C_2H_4]_0$; revised $[F]_{mean} = [F]_0 - 0.825[C_2H_4]_0$ (see eq 13).

molecule^{-1} s^{-1} and $k_1(202\text{ K}) = (1.7 \pm 0.4) \times 10^{-10}$ cm^3 molecule^{-1} s^{-1}. Our previous room-temperature measurement for this reaction[20] was $k_1(298\text{ K}) = (2.7 \pm 0.5) \times 10^{-10}$ cm^3 molecule^{-1} s^{-1}. The reanalyzed data from this study is presented in Table 2 and Figure 3. A linear least-squares analysis of the revised data in Table 2 according to eq 14 gives a bimolecular rate constant of $k_1(298\text{ K}) = (3.0 \pm 0.8) \times 10^{-10}$ cm^3 molecule^{-1} s^{-1}. The intercepts $k_w = +13 \pm 51$, -32 ± 54, and -114 ± 106 s^{-1} at $T = 202$, 236, and 298 K, respectively, are statistically insignificant, thus showing that there are no additional C_2H_4 loss processes in this system. Quoted uncertainties are statistical at the 1σ level plus systematic errors estimated to be about 15%.

Product Branching Studies. The only products of reaction 1 observed at both $T = 202$ and $T = 236$ K were C_2H_3F and C_2H_3. These products are consistent with previous studies.[8,9,16−18,20,21] To determine the product branching fractions, measurements were made by monitoring the C_2H_3F net signal at $m/z = 46$ directly as a function of distance (reaction time). The experiments were conducted with $[C_2H_4]_0 > [F]_0$ to avoid potential loss of C_2H_3F via the secondary reaction 9. $[C_2H_4]_0/[F]_0$ values ranged from 14 to 41. As in the kinetic experiments, molecular oxygen, $[O_2]_0 = (3.6-5.5) \times 10^{14}$ molecule cm^{-3}, was added to scavenge C_2H_3. With $[C_2H_4]_0 = (5.3-6.9) \times 10^{13}$ molecule cm^{-3}, the C_2H_3F signal profile leveled off between $t = 1.1$ and 1.8 ms, indicating that the F + C_2H_4 reaction had gone to completion. At longer reaction times, $t > 2$ ms, the net C_2H_3F signal increased above this constant level. This growth in signal was especially noticeable when the percent dissociation of F_2 in the microwave discharge was <90%, suggesting that atomic hydrogen, formed along with C_2H_3F in reaction 1b, reacts with undissociated F_2

$$H + F_2 \rightarrow HF + F \qquad (15)$$

$$k_{15}(T) = 1.46 \times 10^{-12} \exp(-1210/T)$$
$$\text{cm}^3 \text{ molecule}^{-1} \text{ s}^{-1} \text{ (ref 31)}$$

This reaction, followed by reaction 1, leads to additional C_2H_3F formation. Consequently, only experiments that used CF_4 as a F atom source or had a high F_2 dissociation (and thus low residual $[F_2]$) yielded accurate product branching fractions.

The final product C_2H_3F signal levels were taken as the average of the signals in the plateau region. The magnitudes of the product signals were calibrated using a range of appropriate known concentrations of a reference C_2H_3F/He mixture under similar flow conditions. The product branching fraction, Γ_{1b}, was determined from the equation

$$\Gamma_{1b} = [C_2H_3F]/[F]_0 \qquad (16)$$

For the abstraction channel

$$\Gamma_{1a} = 1 - \Gamma_{1b} \qquad (17)$$

and since C_2H_4F was not detected as a stable product at $P = 1$ Torr, then $\Gamma_{1c} = 0$. The product branching fraction results are summarized in Table 3 and give the following branching fractions: $\Gamma_{1b}(236\text{ K}) = 0.73 \pm 0.20$ and $\Gamma_{1b}(202\text{ K}) = 0.75 \pm 0.16$. Using eq 17 to determine the abstraction channel branching fraction gives $\Gamma_{1a}(236\text{ K}) = 0.27 \pm 0.13$ and $\Gamma_{1a}(202\text{ K}) = 0.25 \pm 0.09$. The quoted uncertainties are statistical at 1σ and include an additional 15% for estimated systematic errors.

At an ionization energy of ~14 eV and $P = 1$ Torr (He), a net signal at $m/z = 47$ was detected at $T = 202$ K. This signal was previously reported in our studies[20] at $T = 298$ K but was unidentified. Two experiments were performed to determine whether the net signal observed at $m/z = 47$ was due to the C_2H_4F addition−stabilization product of reaction 1c. First, simultaneous measurements of both $m/z = 46$ and 47 signals at this low temperature and under the vinyl fluoride yield experimental condition described above showed that the temporal profiles of the two signals matched over the range $2.0 < t < 15.9$ ms. The averaged ratio of $m/z = 47$ to $m/z = 46$ net signal was 0.0233 ± 0.0010. This value is in close agreement with the natural abundance of the ^{13}C isotope in the C_2H_4 reagent (2.2%) and, hence, in the C_2H_3F vinyl fluoride reaction product. Second, further verification of the absence of C_2H_4F was

TABLE 3: Summary of the Experimentally Determined Product Branching Fractions Γ_{1a} and Γ_{1b} at $T = 202$ K and $T = 236$ K for the Reaction F + C_2H_4 → C_2H_3 + HF (1a) and F + C_2H_4 → C_2H_3F + H (1b)

temp K	$[F]_0$[a] 10^{12} molecule cm^{-3}	$[C_2H_4]_0$ 10^{13} molecule cm^{-3}	Γ_{1a}[b]	Γ_{1b}[c]
236	1.11	3.54	0.39	0.61
236	1.11	3.54	0.37	0.63
236	1.78	7.04	0.20	0.80
236	1.78	7.04	0.26	0.74
236	2.58	7.05	0.20	0.80
236	2.58	7.05	0.18	0.82
			$\langle 0.27 \pm 0.13 \rangle$[d]	$\langle 0.73 \pm 0.20 \rangle$[d]
202	1.62	6.60	0.24	0.76
202	1.62	6.60	0.26	0.75
202	1.63	6.57	0.29	0.71
202	1.63	6.48	0.24	0.76
202	2.37	6.58	0.21	0.79
202	2.37	6.49	0.17	0.83
202	2.50	6.59	0.24	0.76
202	2.50	6.59	0.23	0.77
202	4.25[e]	5.94	0.36	0.64
202	4.25[e]	5.94	0.23	0.77
			$\langle 0.25 \pm 0.09 \rangle$[d]	$\langle 0.75 \pm 0.16 \rangle$[d]

[a] Unless noted, F_2 used as F atom precursor. $[O_2]_0 = 4.5 \times 10^{14}$ molecule cm^{-3}. [b] $\Gamma_{1a} = 1 - \Gamma_{1b}$. [c] $\Gamma_{1b} = [C_2H_3F]/[F]_0$. [d] Quoted errors are 1σ statistical plus 15%. Nominal pressure = 1 Torr (He). [e] CF_4 used as F atom precursor. $[O_2]_0 = 5.5 \times 10^{14}$ molecule cm^{-3}.

obtained by the addition of a large excess of O_2 as a scavenger.

$$C_2H_4F + O_2 \rightarrow \text{products} \qquad (18)$$

A signal decrease at $m/z = 47$ was not observed at $[O_2]_0 = 1.5 \times 10^{15}$ molecule cm^{-3} and at $t = 2$ ms. Thus, the $m/z = 47$ signal seen here and in our previous study is not due the presence of the pressure-stabilized free radical adduct C_2H_4F but due to the isotopic vinyl fluoride product $^{13}C_2H_3F$.

Discussion

Arrhenius Expression. The results from this study at low temperatures are combined with the revised $k_1(298\text{ K})$ values using data from our previous study[20] and the previous product branching studies.[21] The rate constants of the two separate channels are obtained from the total rate constant and the corresponding branching fraction, i.e., $k_{1a}(T) = k_1(T)\Gamma_{1a}(T)$ and $k_{1b}(T) = k_1(T)\Gamma_{1b}(T)$ as shown in Table 4. The rate coefficients for reactions 1a and 1b are plotted in Figure 4 as a function of reciprocal temperature, T^{-1}. As can be seen from Figure 4, both the abstraction and the addition channels have rate coefficients that increase with temperature. The lines in Figure 4 are obtained from a linear least-squares analysis of the ln k_{1a} vs T^{-1} and ln k_{1b} vs T^{-1} data; these analyses yield the following Arrhenius expressions:

$$k_{1a}(T) = (7.5 \pm 4.0) \times 10^{-10} \exp[(-1.18 \pm 0.35)/(RT)] \text{ cm}^3\text{ molecule}^{-1}\text{ s}^{-1}$$

$$k_{1b}(T) = (5.2 \pm 1.0) \times 10^{-10} \exp[(-0.57 \pm 0.10)/(RT)] \text{ cm}^3\text{ molecule}^{-1}\text{ s}^{-1}$$

where the errors are quoted at the 1σ plus 15% level and units of kcal mol^{-1} are used for the activation energy.

If the Arrhenius activation energy parameter is used as a barrier energy height, then these results show that the activation barrier for H atom abstraction, $E_{a,absr} = 1.18$ kcal mol^{-1}, is almost twice as large as that for the very fast F + C_2H_6 reaction, $E_{a,absr} = 0.7$ kcal mol^{-1}.[32] Yet the C−H bond in ethylene is stronger than that in ethane by only 10.9 kcal mol^{-1}.[33] Also, the activation barrier for F atom addition, $E_{a,add} = 0.57$ kcal mol^{-1} is only slightly less than the upper limit of 0.8 kcal mol^{-1} established by Robinson et al.[17] in a low-energy crossed molecular beam study.

Alternatively, the temperature dependence of this reaction can be parametrized by a power dependence expression, $k(T) = bT^m$. Applying least-squares analysis to the rate constants given in Table 4 gives

$$k_{1a}(T) = (1.16 \times 10^{-16})T^{2.41} \text{ cm}^3\text{ molecule}^{-1}\text{ s}^{-1}$$

$$k_{1b}(T) = (2.55 \times 10^{-13})T^{1.17} \text{ cm}^3\text{ molecule}^{-1}\text{ s}^{-1}$$

This power dependence expression for k_{1b} may be preferred over the Arrhenius expression because of the absence of an energy barrier at the entrance of the potential energy surface for the F + C_2H_4 system.[17]

RRKM Model. The observed branching ratio, k_{1c}/k_{1b}, can be used to provide information on the thermokinetics for the addition−decomposition reactions. The addition of F to C_2H_4 and its subsequent decomposition (D) to H + C_2H_3F or stabilization (S) to C_2H_4F can be modeled as a simple chemical activation system[34] in which the adduct is formed with an internal energy distribution of populated states.

$$F + C_2H_4 \rightarrow C_2H_4F(E), \quad k_f \qquad (1b')$$

$$C_2H_4F(E) \rightarrow H + C_2H_3F, \quad D, \quad k(E) \qquad (1b'')$$

$$C_2H_4F(E) \rightarrow F + C_2H_4, \quad D', \quad k'(E) \qquad (-1b')$$

$$C_2H_4F(E) + M \rightarrow C_2H_4F(E') + M, \quad S, \quad k_2(E',E) \qquad (1c')$$

where k_f is the rate coefficient for the formation reaction, $k(E)$ and $k'(E)$ are the microscopic unimolecular rate coefficients for decompositions, and $k_2(E',E)$ is the rate coefficient for intermolecular energy from internal energy E to E'. A potential energy profile with defining energies is exhibited in Figure 5. The critical energies are designated as either E_0 or $E_0(X)$, while reaction energy changes are designated by ΔE_0^0(reactant;product). The excess energy E^+ is the internal energy of the transition state and is the difference between the internal energy of reactant and the critical energy for reaction, i.e. $E^+ = E - E_0$; the minimum excess energy, E^+_{min} is the difference in critical energies: $E^+_{min} = E_0' - E_0$. The $k(E)$'s can be computed with the RRKM model,[35]

$$k(E) = \frac{r^+}{h}\frac{Q^+}{Q}\frac{\sum P(\epsilon^+)}{\rho(E)}$$

where r^+ is the reaction path degeneracy, Q^+/Q is the adiabatic partition function ratio for rotations, $\sum P(\epsilon^+)$ is the sum of all active internal energy eigenstates of the transition complex with total energy E^+, and $\rho(E)$ is the density of states for the energized reactant with energy E. If the addition product is formed by thermalized reactants, then the distribution of internal energy states for C_2H_4F is given by[36]

$$f(E) = \frac{k'(E)\,B(E)}{\sum k'(E)\,B(E)} \qquad \text{for } E = E_0' \text{ to } \infty$$

where $B(E)$ is the Boltzmann distribution

$$B(E) = \frac{\rho(E)\exp(-E/(RT))}{\sum \rho(E)\exp(-E/(RT))} \qquad \text{for } E = 0 \text{ to } \infty$$

TABLE 4: Summary of Values for $k_1(T)$ and Product Branching Fractions for the $F(^2P) + C_2H_4$ Reaction

temp K	k_1[a]/10^{-10} cm^3 molecule^{-1} s^{-1}	Γ_{1a}[b]	Γ_{1b}[c]	k_{1a}[d]/10^{-11} cm^3 molecule^{-1} s^{-1}	k_{1b}[d]/10^{-10} cm^3 molecule^{-1} s^{-1}
298	3.0 ± 0.8[e]	0.35 ± 0.04[f]	0.65 ± 0.06[f]	10.6 ± 2.8	1.97 ± 0.54
236	2.1 ± 0.5[g]	0.27 ± 0.13[g]	0.73 ± 0.20[g]	5.6 ± 1.6	1.51 ± 0.57
202	1.7 ± 0.4[g]	0.25 ± 0.09[g]	0.75 ± 0.16[g]	4.2 ± 1.1	1.25 ± 0.41

[a] Quoted uncertainties are statistical at one standard deviation plus 15% for systematic errors. [b] Γ_{1a} is the branching fraction for the abstraction product channel forming $C_2H_3 + HF$. [c] Γ_{1b} is the branching fraction for the addition product channel forming $C_2H_3F + H$. [d] The combined uncertainties in k_{1a} and k_{1b} are calculated as the product of the absolute k values and the relative combined uncertainty values. The relative combined uncertainty values are obtained as the square root of the sum of the squares of the individual relative uncertainties. [e] Reanalysis of data from ref 20 as discussed in text and reported in Table 2. [f] Reference 21; quoted uncertainties are at 10%. [g] This study. Quoted uncertainties are statistical at one standard deviation plus 15% for systematic errors.

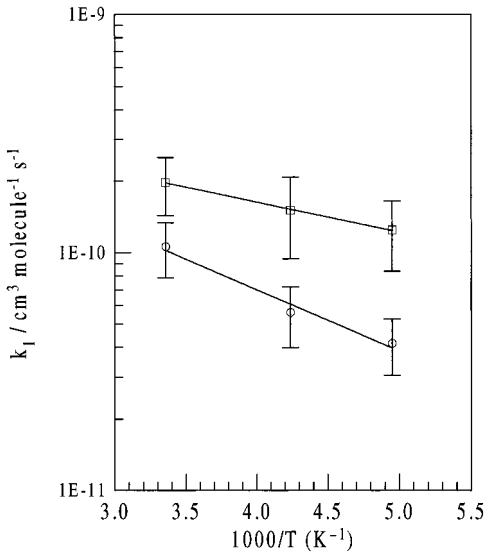

Figure 4. Arrhenius plot for the $F(^2P) + C_2H_4$ reaction. Separate plots are shown for the H abstraction channel (open circles), k_{1a}, and for the addition−decomposition channel (open squares), k_{1b}. Solid lines are obtained from linear least-squares analyses of the ln k_{1a} vs T^{-1} and the ln k_{1b} vs T^{-1} data and yield the Arrhenius expressions given in the text. Error bars indicate $\pm 1\sigma$ plus 15% for both k_{1a} and k_{1b}.

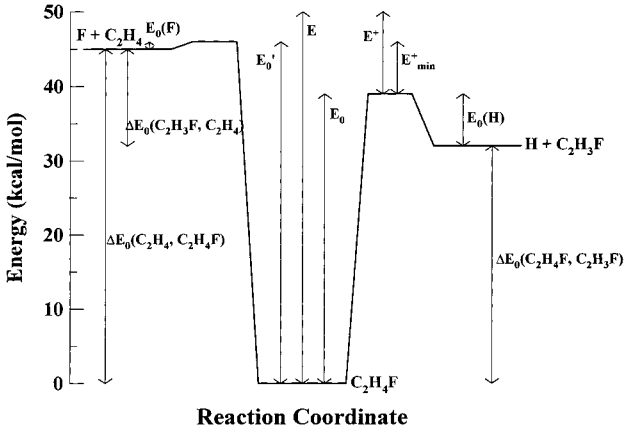

Figure 5. Potential energy profile for C_2H_4F system depicting energies for reactants, intermediates, transition states, and products.

In these experiments the deactivator (M), helium, is known to be a weak collider;[37] i.e., helium does not remove sufficient energy from C_2H_4F to completely quench reactions 1b″ and −1b′. The strong collision assumption requires that stabilization is the result of a single collision. Thus, for a weak collider, stabilization results from sequential collisions; at low collision rates, i.e., low pressures, the unimolecular processes are enhanced.

The populations can be calculated by solving the master equation

$$\mathrm{d}[N(E)]/\mathrm{d}t = f(E) + \sum k(E,E')[\mathrm{M}][N(E')] - \sum k(E',E)[\mathrm{M}][N(E)] - k(E)[N(E)] - k'(E)[N(E)]$$

for all E. For steady-state conditions, all $\mathrm{d}[N(E)]/\mathrm{d}t = 0$, the resulting coupled algebraic equations can be solved for $[N(E)]_{ss}$.[38] The steady-state populations can then be used to calculate the branching ratios, i.e., S/D and D'/D.

$$S = \sum k(E',E)[N(E)]_{ss} \qquad \text{for all } E \geq E_0 \text{ and } E' < E_0$$

$$D = \sum k(E)[N(E)]_{ss} \qquad \text{for all } E \geq E_0$$

$$D' = \sum k'(E)[N(E)]_{ss} \qquad \text{for all } E \geq E_0'$$

$$S + D + D' = 1$$

Thus, the amounts of decomposition and stabilization can be calculated from the $k(E)$'s and the Boltzmann distribution at ambient temperature and pressure.

To calculate the $k(E)$'s, vibrational frequencies and moments of inertia for the transition states and C_2H_4F radical must be known. There are no direct experiments; however, ab initio calculations for the radical and transition states have been reported.[39] In the present kinetic calculations the previously reported vibrational frequencies and geometries were used; the energetics were optimized with respect to the present experimental observations.

The details of $k(E',E)$ are not known a priori; often the observed pressure dependence of S/D or D'/D is used to parametrize $k(E',E)$. Typically, three parameters are used to parametrize $k(E',E)$:[40] the Lennard-Jones collision frequency (σ and ϵ), the shape of the energy-transfer distribution (exponential, Gaussian, or step ladder), and the average energy removed per collision, $\langle \Delta E_d \rangle$. An exponential model is often chosen for weak colliders such as the rare gases, and the Lennard-Jones collision parameters can be estimated. There are no reported values for $\langle \Delta E_d \rangle$ in the C_2H_4F system; however, an estimate can be made by comparing similar systems, i.e. radicals with similar excitation and critical energies. The chemically activated ethyl[41] and butyl[42] radicals with ~40 kcal mol^{-1} of internal energy are formed by the addition of H to the appropriate olefin. The critical energies for decomposition are 40 and 33 kcal mol^{-1} for the ethyl and butyl radicals, respectively. The reported results indicate that $\langle \Delta E_d \rangle$ for helium is independent of temperature between 78 and 300 K and is ~400 cm^{-1}. The Michael group[43−45] has also extensively studied and performed RRKM calculations on chemically activated ethyl radicals. However, their strong collider calculations used a pressure-independent collisional efficiency factor for helium, i.e. simple pressure displacement. Thus, their calculations did not include a collisional deactivation cascade; this is important for low-pressure systems.

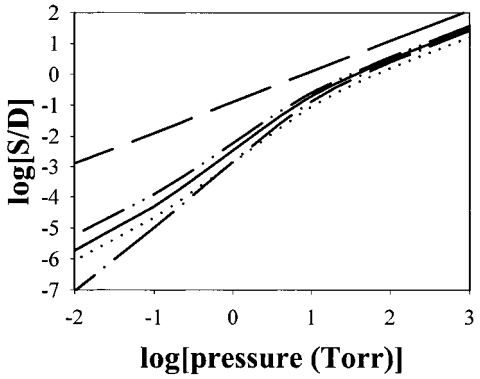

Figure 6. Plots of log(*S*/*D*) vs log(pressure) at 202 K for strong collider (dashed line) for exponential models with $\langle\Delta E_d\rangle = 327$ (dashed−dotted line), 414 (solid line), and 498 (dash−dot−dotted line) cm^{-1} and for the 414 exponential model at 298 K (dotted line). The critical energies are $E_0 = 38.2$ kcal mol^{-1} and $E_0' = 46.0$ kcal mol^{-1} with $E^+_{min} = 7.8$ kcal mol^{-1}.

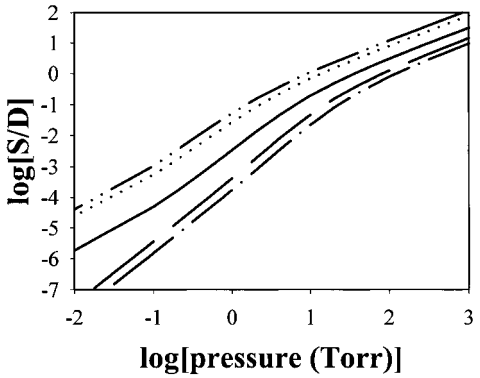

Figure 7. Plots of log(*S*/*D*) vs log(pressure) at $T = 202$ K for an exponential model with $\langle\Delta E_d\rangle = 414$ cm^{-1}: $E_0' = 46.0$ kcal mol^{-1} with $E_0 = 40.2$ (dashed−dot−dotted line), 38.2 (solid line), and 36.2 (dash−dotted line) kcal mol^{-1} and $E_0 = 38.2$ kcal mol^{-1} with $E_0' = 44.0$ (dotted line) and $E_0' = 48.0$ (dashed line) kcal mol^{-1}.

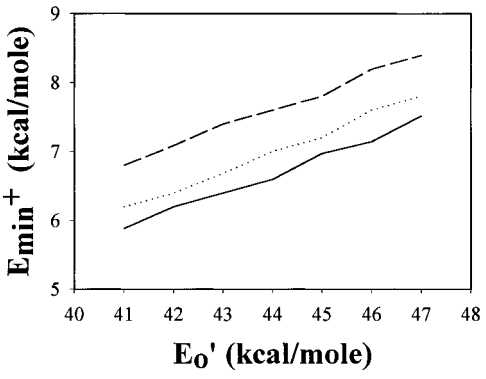

Figure 8. Plots of E^+_{min} vs E_0' for three values of *S*/*D*: *S*/*D* = 0.008 (solid line), 0.005 (dotted line), and 0.002 (dashed line).

The results of the steady-state calculations are summarized in Figures 6−9. The effect of the dependence of *S*/*D* on pressure, temperature, and $\langle\Delta E_d\rangle$ is shown in Figure 6. For all collision models (strong collider and exponential models with $\langle\Delta E_d\rangle$ of 327, 414, and 498 cm^{-1}) *S*/*D* decreases with decreasing pressure; the strong collider exhibits near-linearity over the whole pressure range, while *S*/*D* for the weak colliders exhibit a large deviation from the strong collider as the pressure decreases. At high pressures (>100 Torr) a scale factor (collisional efficiency) of ~0.2 can be used in converting the weak collider pressure to an effective strong collider pressure. However, below 100 Torr, the collision efficiency is pressure-dependent; at 1 Torr the

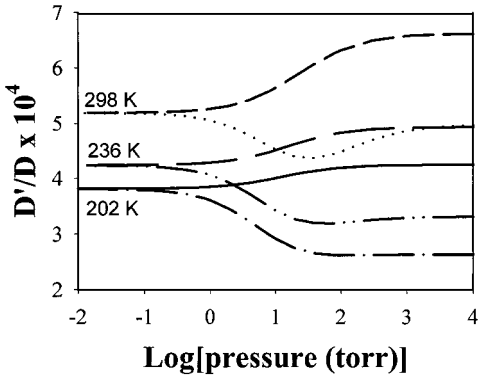

Figure 9. Plots of *D*′/*D* vs log(pressure) as a function of temperature for a strong collider: $T = 202$ K (solid line), 236 K (long dashed line), and 298 K (short dashed line). Similar plots for an exponential model with $\langle\Delta E_d\rangle = 414$ cm^{-1} as a function of temperature are also shown: $T = 202$ K (dashed−dotted line), 236 K (dash−dot−dotted line), and 298 K (dotted line). The critical energies are $E_0 = 38.2$ kcal mol^{-1} and $E_0' = 46.0$ kcal mol^{-1} with $E^+_{min} = 7.8$ kcal mol^{-1}.

collision efficiency is <0.01. Also to be noted is that for all pressures a decrease in ambient temperature produces an increase in *S*/*D*; thus, in this work where an upper limit for *S* of 0.005 is reported (i.e., $S/D \approx 5 \times 10^{-3}$, since $D \approx 1$) the lowest temperature (202 K) is used for the comparison. A change in *S*/*D* with decreasing temperature is due to two effects: the collision number and the average energy of reacting radicals. A decrease in temperature produces a net increase in the collision frequency, which results in an *increase* of *S*/*D*, while a decrease in temperature also reduces the average energy of radicals so that fewer "weak" collisions are required for stabilization, i.e., *S*/*D increases* with decreasing temperature for a constant $\langle\Delta E_d\rangle$. Thus, both factors predict that *S*/*D* will *increase* with decreasing temperature.

The dependence of *S*/*D* vs pressure at 202 K on E_0 and E_0' are shown in Figure 7. An increase in E_0' or a decrease in E_0 decreases *S*/*D*. There are a number of combinations of E_0 and E_0' that are consistent with the upper limit for the experimental observation; in fact, only an upper limit of E_0 for a given E_0' or a lower limit of E_0' for a given E_0 can be estimated. In Figure 8 a plot of E^+_{min} vs E_0' for three values of *S*/*D* (0.002, 0.005, 0.008) is shown; for the present experimental conditions $S/D \approx S$, since $D \approx 1$. For the indicated range of *S*/*D* these plots illustrate that *S*/*D* is more sensitive to E^+_{min} than it is to E_0'. To maintain a constant *S*/*D*, a change in E^+_{min} of 1 kcal mol^{-1} is equivalent to a change of 4.5 kcal mol^{-1} in E_0'. Thus, the present experiments can provide an estimate for E^+_{min}.

By use of reported values for enthalpies of formation at 0 K for F, C_2H_4, H, and C_2H_3F, $\Delta E_0^0 = 13.0$ kcal mol^{-1} and the best estimate for $E_0' = 46$ kcal mol^{-1} gives $E^+_{min} > 7$ kcal mol^{-1}. From the potential energy profile, it can be seen that

$$E^+_{min} = E_0(F) - E_0(H) + \Delta E_0^0(C_2H_4;C_2H_3F)$$

so that

$$E_0(H) - E_0(F) = \Delta E_0^0(C_2H_4;C_2H_3F) - E^+_{min} < 6 \text{ kcal mol}^{-1}$$

or with $E_0(F) = 1$ kcal mol^{-1}, then

$$E_0(H) = E_0(F) + \Delta E_0^0(C_2H_4;C_2H_3F) - E^+_{min} < 7 \text{ kcal mol}^{-1}$$

Thus, the critical energy for H addition to C_2H_3F is less than 6 kcal mol^{-1} larger than that for the addition of F to C_2H_4, i.e., the electronegative fluorine atom reduces the π electron density and thus increases the critical energy for addition by less than 6 kcal mol^{-1}.

These energetics also predict the pressure dependence of D'/D as a function of temperature as shown in Figure 9. For a given pressure, D'/D increases with increasing temperature. This is understood, since the average energy of reacting molecules increases with increasing temperature and the change in the slope of $k(E)$ with energy increases more for reaction $-1b'$ than it does for 1b″. The pressure dependence of D'/D is more complex; it involves both the increase of the average energy of reacting molecules with increasing pressure, which favors D' and the increase in steady-state population below E_0', which favors D. At 1 Torr of helium these effects cancel one another and it is also observed that D'/D is nearly independent of the energy-transfer model and D'/D increases from 7×10^{-4} at 202 K to 1.5×10^{-3} at 298 K. Thus, reaction $-1b'$ is unimportant. Details of this reaction could be obtained by studying the addition of F to *cis*-$C_2H_2D_2$ or *trans*-$C_2H_2D_2$.

Comparison of the Reactions of F, Cl, and CN with C_2H_4. For any new kinetic results for an elementary reaction, it is valuable to compare the new results to different but related reactions. As discussed in our previous paper,[20] the reaction of F with C_2H_4 is not analogous to the reactions of the other halogen atoms Cl and Br with ethylene. For these reactions, until recently, only the pressure-stabilized adducts C_2H_4Cl[46−48] or C_2H_4Br[48,49] were reported as products. Thermochemical calculations based on a heat of formation of the vinyl radical of 70.6 kcal mol^{-1} (ref 47) show that the addition−decomposition channel and the abstraction channel are endothermic for these reactions. Recently, however, low-pressure experiments ($P = 0.2-20$ Torr) by Kaiser and Wallington[47] and by Pilgrim and Taatjes[50] have verified the presence of an abstraction channel in the Cl + C_2H_4 reaction

$$Cl + C_2H_4 \rightarrow C_2H_3 + HCl \qquad (19a)$$

and have measured a rate coefficient at $T = 297-383$ K.

$$k_{19a}(T) = 6.0 \times 10^{-11} \exp(-3270/T)$$
$$\text{cm}^3 \text{ molecule}^{-1} \text{ s}^{-1} \text{ (ref 47)}$$

H atom abstraction is the minor channel for both Cl + C_2H_4 and F + C_2H_4. For Cl + C_2H_4, the abstraction channel has a branching fraction of only 0.0035 at $P = 1$ Torr, whereas it is 0.35 for F + C_2H_4, a 100-fold difference.[21]

Since both the abstraction and the addition−decomposition channel are endothermic in the Cl + C_2H_4 reaction, the addition−stabilization channel is dominant at $P > 3$ mTorr

$$Cl + C_2H_4 (+M) \rightarrow C_2H_4Cl (+M) \qquad (19b)$$

Kaiser and Wallington[47] have reported a limiting high-pressure rate coefficient for Cl + C_2H_4 of $k_{\infty,19} = 5.7 \times 10^{-10}$ cm^3 molecule^{-1} s^{-1}, which is almost a factor of 2 faster than the total rate constant for F + C_2H_4, $k_1 = 3.0 \times 10^{-10}$ cm^3 molecule^{-1} s^{-1} at $T = 298$ K. The only effect of pressure in the F + C_2H_4 system will be on the partitioning between addition−decomposition (reaction 1b) and addition−stabilization (reaction 1c). This results from the observation that k(addition)/k(total) for F + C_2H_4 is 0.65 in 4000 Torr of SF_6[9] and in 0.7 Torr of He[19] and is ∼0.75 in 2×10^{-4} Torr of C_2H_4.[13]

Perhaps a better, but not perfect, analogue of the F atom is the cyano radical, CN, often referred to as a pseudo-halogen[51] because of its high electron affinity (3.86 eV, ref 52), which is comparable to that of F (3.40 eV, ref 53). There have been numerous kinetic studies on the CN + C_2H_4 reaction,[54−62] but there has been only one product branching fraction study.[63] As in the F + C_2H_4 reaction, the total rate of this reaction has been found to be independent of total pressure.[56,59,60,62] However, a comparison of the temperature dependency of these two reaction rates shows major differences. In contrast to the CN + C_2H_4 reaction, which has a reported E_a of −0.34 kcal mol^{-1} (ref 62), we have observed a positive temperature dependence in the F + C_2H_4 reaction overall as well as separately in the abstraction channel and in the addition channel. There are significant differences in the mechanisms between the F + C_2H_4 and the CN + C_2H_4 reactions in the partitioning between the abstraction and the addition−decomposition channels. While the total rate coefficient at $T = 298$ K for both reactions are almost the same, $k_1(298\text{ K}) = 3.0 \times 10^{-10}$ cm^3 molecule^{-1} s^{-1} and $k_{20}(298\text{ K}) = 2.5 \times 10^{-10}$ cm^3 molecule^{-1} s^{-1} (average of seven studies; refs 56−62), the product branching fractions for the addition−decomposition channels ($\Gamma_{\text{add.}-\text{decomp}}$) are quite different. For the F reaction, $\Gamma_{\text{add.}-\text{decomp}}$ is 0.65 but only 0.20 for the CN reaction.[63] The F atom reaction occurs via two parallel processes: direct H atom abstraction (reaction 1a) and addition to the C−C double bond (reactions 1b and 1c).[8,16,19] For the CN reaction, all products are suggested to arise from a single activated complex,[60,63] i.e.,

$$CN + C_2H_4 \rightarrow [C_2H_4{-}CN]^* \rightarrow C_2H_3 + HCN \qquad (20a)$$
$$\rightarrow [C_2H_4{-}CN]^* \rightarrow C_2H_3CN + H \qquad (20b)$$

Evidence for this mechanism is twofold. First, all four temperature-dependent rate studies[59−62] observed a slightly negative temperature dependence ultimately down to $T \approx 50$ K[61] and a pressure independence up to $P = 500$ Torr of Ar.[62] Second, even though the C−H bond strength is larger in C_2H_2 than in C_2H_4, the overall rate coefficients for both CN + C_2H_4 and CN + C_2H_2 are identical over the temperature range $T = 100-704$ K.[59−62]

Conclusion

The primary results of this study are threefold. First, the data from our discharge flow mass spectrometry experiments at low temperatures show that the F + C_2H_4 rate constant increases with temperature. If an Arrhenius expression is used to fit the data, activation barriers of 1.2 and 0.6 kcal mol^{-1} are observed for the H atom abstraction and the F atom addition channels, respectively.

The second conclusion is that the branching fraction for the addition−decomposition channel increases only marginally with a decrease in temperature. Also, the addition−stabilization product, C_2H_4F, was not observed at low temperatures and at $P = 1$ Torr. Thus, the F + C_2H_4 reaction can be used as a convenient laboratory source of C_2H_3 radicals at low temperatures if one recognizes complications from the production via reaction 1b of hydrogen atoms that can react rapidly with C_2H_3.

Finally, we have shown via RRKM calculations that the critical energy for H addition to C_2H_3F is less than 6 kcal mol^{-1} larger than that for the addition of F to C_2H_4 and that the competitive decomposition of chemically activated C_2H_4F radicals favors C−H bond rupture by a factor greater than 1000 over that for C−F bond rupture.

Acknowledgment. R.P.T. and F.L.N. acknowledge the support of NASA Cooperative Agreement NCC5-68 to the Catholic University of America and the NASA Planetary Atmospheres Program. All authors thank Dr. Louis J. Stief for the use of laboratory facilities and for helpful discussions.

References and Notes

(1) Yung, Y. L.; Allen, M.; Pinto, J. P. *Astrophys. J., Suppl. Ser*. **1984**, *55*, 465. Lara, L. M.; Lellouch, E.; Lopez-Moreno, J. J.; Rodrigo, R. *J. Geophys. Res.* **1996**, *101*, 23261. Romani, P. N.; Bishop, J.; Bézard, B.; Atreya, S. *Icarus* **1993**, *106*, 442.

(2) Tsang, W.; Hampson, R. F. *J. Phys. Chem. Ref. Data* **1986**, *15*, 1087.

(3) Herbst, E.; Leung, C. M. *Mon. Not. R. Astron. Soc.* **1986**, *222*, 689. Herbst, E.; Leung, C. M. *Astrophys. J., Suppl. Ser*. **1989**, *69*, 271.

(4) Payne, W. A.; Stief, L. J. *J. Chem. Phys*. **1976**, *64*, 1150.

(5) Jones, W. E.; Skolnik, E. G. *Chem Rev.* **1976**, *76*, 562.

(6) Fettis, G. C.; Knox, J. H. *Prog. React. Kinet*. **1964**, *2*, 2.

(7) Maricq, M. M.; Szente, J. J. *J. Phys. Chem.* **1994**, *98*, 2078.

(8) Parson, J. M.; Lee, Y. T. *J. Chem. Phys*. **1972**, *56*, 4658.

(9) Williams, R. L.; Rowland, F. S. *J. Phys. Chem.* **1972**, *76*, 3509.

(10) Flores, A. L.; deB. Darwent, B. *J. Phys. Chem*. **1969**, *73*, 2203.

(11) Benson, S. W. *Thermochemical Kinetics*, 2nd ed.; J. Wiley and Sons: New York, 1976.

(12) Moehlmann, J. G.; Gleaves, J. T.; Hudgens, J. W.; McDonald, J. D. *J. Chem. Phys*. **1974**, *60*, 4790.

(13) Moehlmann, J. G.; McDonald, J. D. *J. Chem. Phys*. **1975**, *62*, 3061.

(14) Bogan, D. J.; Setser, D. W. *J. Chem. Phys*. **1976**, *64*, 586.

(15) Donaldson, D. J.; Watson, D. G.; Sloan, J. J. *Chem. Phys.* **1982**, *68*, 95.

(16) Farrar, J. M.; Lee, Y. T. *J. Chem. Phys.* **1976**, *65*, 1414.

(17) Robinson, G. N.; Contininette, R. E.; Lee, Y. T. *J. Chem. Phys*. **1990**, *92*, 275.

(18) Milstein, R.; Williams, R. L.; Rowland, F. S. *J. Phys. Chem.* **1974**, *78*, 857.

(19) Smith, D. J.; Setser, D. W.; Kim, K. C.; Bogan, D. J. *J. Phys. Chem.* **1977**, *81*, 898.

(20) Nesbitt, F. L.; Monks, P. S.; Scanlon, M.; Stief, L. J. *J. Phys. Chem*. **1994,** *98*, 4307.

(21) Slagle, I. R.; Gutman, D. *J. Phys. Chem.* **1983**, *87*, 1818.

(22) Brunning, J.; Stief, L J. *J. Chem. Phys.* **1986**, *84*, 4371.

(23) Appelman, E. H.; Clyne, M. A. A. *J. Chem. Soc., Faraday Trans. 1* **1975**, *71*, 2072.

(24) Marston, G.; Nesbitt, F. L.; Nava, D. F.; Payne, W. A.; Stief, L. J. *J. Phys. Chem.* **1989**, *93*, 5769.

(25) Lias, S. G.; Bartmess, J. E.; Liebman, J. F.; Holmes, J. L.; Levin, R. D.; Mallard, W. G. *J. Phys. Chem. Ref. Data* **1988**, *17* (Suppl. 1).

(26) Lewis, R. S.; Sander, S. P.; Wagner, W.; Watson, R. T. *J. Phys. Chem.* **1980**, *84*, 2009.

(27) Thorn, R. P.; Payne, W. A.; Stief, L. J.; Tardy, D. C. *J. Phys. Chem* **1996**, *100*, 13594.

(28) Slagle, I. R.; Park, J.-Y.; Heaven, M. C.; Gutman, D. *J. Am. Chem. Soc*. **1984**, *160*, 4356. Krueger, H.; Weitz, E. *J. Chem. Phys.* **1988**, *88*, 1608.

(29) Baulch, D. L.; Cobos, C. J.; Cox, R. A.; Frank, P.; Hayman, G.; Just, Th.; Kerr, J. A,; Murrells, T.; Pilling, M. J.; Troe, J.; Walker, R. W.; Warnatz, J. *J. Phys. Chem. Ref. Data* **1995**, *24*, 1609.

(30) Iyer, R. S.; Chen, C.-Y.; Rowland, F. S. *J. Phys. Chem.* **1985**, *89*, 2042.

(31) Baulch, D. L.; Duxbury, J.; Grant, S. J.; Montague, D. C. *J. Phys. Chem Ref. Data, Suppl.* **1981** *10*, 1.

(32) Maricq, M. M.; Szente, J. J. *J. Phys. Chem* **1994**, *98*, 2078.

(33) NIST Webbook, http://webbook.nist.gov.

(34) Rabinovitch, B. S.; Flowers, M. C. *Q. Rev.* **1964**, *18*, 122.

(35) (a) Marcus, R. A.; Rice, O. K. *J. Phys. Colloid Chem*. **1951**, *55*, 894. (b) Marcus, R. A. *J. Chem. Phys.* **1952**, *20*, 359.

(36) Rabinovitch, B. S.; Diesen, R. W. *J. Chem. Phys*. **1959**, *30*, 735.

(37) Tardy, D. C.; Rabinovitch, B. S. *Chem. Rev.* **1977**, *77*, 369.

(38) Tardy, D. C.; Rabinovitch, B. S. *J. Chem. Phys*. **1968**, *48*, 5194.

(39) (a) Schlegel, H. B. *J. Phys. Chem.* **1982**, *86*, 4878. (b) Schlegel, H. B.; Bhalla, K. C.; Hase, W. L. *J. Phys. Chem*. **1982**, *86*, 4883.

(40) Oref, I.; Tardy, D. C. *Chem. Rev*. **1990**, *90*, 1407.

(41) Current, J. H.; Rabinovitch, B. S. *J. Chem. Phys*. **1964**, *40*, 2742.

(42) Kohlmaier, G.; Rabinovitch, B. S. *J. Chem. Phys.* **1963**, *38*, 1692, 1709.

(43) Michael, J. V.; Suess, G. N. *J. Chem. Phys*. **1973**, *58*, 2807.

(44) Cowfer, J. A.; Michael, J. V. *J. Chem. Phys*. **1975**, *62*, 3504.

(45) Lee, J. H.; Michael, J. V.; Payne, W. A.; Stief, L. J. *J. Chem. Phys*. **1978**, *68*, 1817.

(46) Maricq, M. M.; Szente, J. J.; Kaiser, E. W. *J. Phys. Chem*. **1993**, *97*, 7970.

(47) Kaiser, E. W.; Wallington, T. J. *J. Phys. Chem*. **1996**, *100*, 4111.

(48) Yarwood, G.; Peng, N.; Niki, H. *Int. J. Chem. Kinet*. **1992**, *24*, 369.

(49) Barnes, I.; Bastian, K. H.; Overath, R.; Tong, Z. *Int. J. Chem. Kinet*. **1989**, *21*, 499.

(50) Pilgrim, J. S.; Taatjes, C. A. *J. Phys. Chem. A* **1997**, *101*, 4172.

(51) Bersohn, R. In *Molecular Energy Transfer*; Levine, R. D., Jortner, J., Eds.; Wiley: New York, 1976; p 154.

(52) Bradforth, S. E.; Kim, E. H.; Arnold, D. W.; Neumark, D. M. *J. Chem. Phys*. **1993**, *98*, 800.

(53) Blondel, C.; Cacciani, P.; Delsort, C.; Trainham, R. *Phys. Rev. A* **1989**, *40*, 3698.

(54) Bullock, G. E.; Cooper, R. *J. Chem. Soc., Faraday Trans. 1* **1971**, *67*, 3258.

(55) Schacke, H.; Wagner, H. G.; Wolfrum, J. *Ber. Bunsen-Ges. Phys. Chem*. **1977**, *81*, 670.

(56) Lichtin, D. A.; Lin, M. C. *Chem. Phys.* **1985**, *96*, 473.

(57) Sayad, N.; Li, X.; Caballer, J. F.; Jackson, W. M. *J. Photochem. Photobiol., A* **1988**, *45*, 177.

(58) North, S. W.; Fei, R.; Sears, T. J.; Hall, G. *Int. J. Chem. Kinet*. **1996**, *29*, 127.

(59) Lichtin, D. A.; Lin, M. C. *Chem. Phys.* **1986**, *104*, 325.

(60) Herbert, L.; Smith, I. W. M.; Spencer-Smith, R. D. *Int. J. Chem. Kinet*. **1992**, *24*, 791.

(61) Sims, I. R.; Queffelec, J.-L.; Traver, S.; Rowe, B. R.; Herbert, L. B.; Karthäuser, J.; Smith, I. W. M. *Chem. Phys. Lett.* **1993**, *211*, 461.

(62) Yang, D. L.; Yu, T.; Wang, N. S.; Lin, M. C. *Chem. Phys*. **1992**, *160*, 317.

(63) Monks, P. S.; Romani, P. N.; Nesbitt, F. L.; Scanlon, M.; Stief, L. J. *J. Geophys. Res.* **1993**, *98*, 17115.